The Astronomical Journal, 161:107 (16pp), 2021 March https://doi.org/10.3847/1538-3881/abd703

The ANTARES Astronomical Time-domain Event Broker

Thomas Matheson[1], Carl Stubens[1], Nicholas Wolf[1], Chien-Hsiu Lee (李見修)[1], Gautham Narayan[2,3], Abhijit Saha[1], Adam Scott[1], Monika Soraisam[2,4], Adam S. Bolton[1], Benjamin Hauger[1], David R. Silva[5], John Kececioglu[6], Carlos Scheidegger[6], Richard Snodgrass[6], Patrick D. Aleo[2], Eric Evans-Jacquez[6,7], Navdeep Singh[6,8], Zhe Wang[6], Shuo Yang[6,9], and Zhenge Zhao[6]

[1] NSF's National Optical-Infrared Astronomy Research Laboratory, 950 North Cherry Avenue, Tucson, AZ 85719, USA; tom.matheson@noirlab.edu
[2] Department of Astronomy, University of Illinois at Urbana-Champaign, Urbana, IL 61801, USA
[3] Center for Astrophysical Surveys, National Center for Supercomputing Applications, Urbana, IL 61801, USA
[4] National Center for Supercomputing Applications, University of Illinois at Urbana-Champaign, Urbana, IL 61801, USA
[5] University of Texas at San Antonio College of Sciences, One UTSA Circle, San Antonio, TX 78249, USA
[6] Department of Computer Science, The University of Arizona, 1040 East 4th Street, Tucson, AZ 85721, USA
[7] Wisconsin IceCube Particle Astrophysics Center, University of Wisconsin-Madison, Madison, WI 53703 USA
[8] Amazon.com, Inc., 440 Terry Avenue North, Seattle, WA 98109, USA
[9] DiDi Research America, 450 National Avenue, Mountain View, CA 94043, USA

Received 2020 July 9; revised 2020 December 21; accepted 2020 December 22; published 2021 February 8

Abstract

We describe the Arizona-NOIRLab Temporal Analysis and Response to Events System (ANTARES), a software instrument designed to process large-scale streams of astronomical time-domain alerts. With the advent of large-format CCDs on wide-field imaging telescopes, time-domain surveys now routinely discover tens of thousands of new events each night, more than can be evaluated by astronomers alone. The ANTARES event broker will process alerts, annotating them with catalog associations and filtering them to distinguish customizable subsets of events. We describe the data model of the system, the overall architecture, annotation, implementation of filters, system outputs, provenance tracking, system performance, and the user interface.

Unified Astronomy Thesaurus concepts: Time domain astronomy (2109); Astronomy software (1855); Computational methods (1965); Astronomical methods (1043)

1. Introduction

The practice of time-domain astronomy is undergoing immense changes. The pathway for the detection of transient and variable objects in the sky once relied on visual inspection and comparison of images. The advent of digital detectors, especially large-format CCDs that can be deployed on wide-field telescopes, has enabled a new era where image subtraction algorithms can identify virtually every difference between a current image and a template over thousands of square degrees of sky each night.

As an illustration of the change in scale, there were 4038 International Astronomical Union Circulars (IAUCs) issued between 1991 January and 2010 December with 10,358 entries. Some of those entries were for multiple objects, but the vast majority were single events, sometimes for follow-up observations of prior discoveries. Even if we make the generous assumption of ∼2 unique objects per IAUC entry, the main worldwide channel for information about transients and variables had ∼20,000 events over two decades, averaging fewer than three per day. The Zwicky Transient Facility (ZTF; Bellm et al. 2019; Graham et al. 2019; Masci et al. 2019) uses a 47 deg^2 imager on the Palomar 48-inch telescope to perform a time-domain survey. The public portion of the ZTF survey (40% of the time) generates several hundred thousand alerts (any object that has changed significantly in brightness or position) each night and thus outperforms those two recent decades in less than an hour.

On the not-too-distant horizon is the Legacy Survey of Space and Time (LSST; Ivezić et al. 2019; Kantor 2014; Kahn 2018) that will be carried out at the Vera C. Rubin Observatory. With a 10 deg^2 camera and 8.4 m mirror (effective aperture 6.7 m), the Rubin Observatory will be able to observe a wide, fast, and deep survey of the southern sky. Each LSST image is anticipated to have ∼10,000 objects that have changed in brightness or position at a significance of 5σ. With ∼1000 pointings per night, LSST will generate ∼10,000,000 time-domain alerts every night for the 10 yr duration of the survey. Many of these will be repetitions of periodic variables or known solar system objects (e.g., Ridgway et al. 2014), but even 10% of the LSST rate will be enormous. Hidden among these unknown events will be rare and unusual objects, some never seen before and some with short lifetimes. Without an efficient software infrastructure to filter these alerts, the events that generated them will remain undiscovered. Building such a system has been a high priority for national committees concerned with maximizing the science potential of LSST (e.g., National Research Council 2015; Najita et al. 2016), and this led to the development of a software infrastructure system that can process a large volume of alerts efficiently and rapidly. In 2013, astronomers at the National Optical Astronomy Observatory (NOAO) and computer scientists from the University of Arizona began to create this tool, now named the Arizona-NOIRLab Temporal Analysis and Response to Events System (ANTARES).

A system that acts as an intermediary between sources of information and the consumer in the commercial world has come to be known as a broker, with a stockbroker being perhaps the most common example. This term has been adopted by the astronomical community (e.g., Borne 2008), so ANTARES and systems like it are often referred to as alert brokers (or, simply, brokers). For a summary of prior work in brokering, see Section 2.3 of Narayan et al. (2018). Other broker systems include Make Alerts Really Simple (MARS),[10]

[10] https://Mars.lco.global/

Lasair (Smith et al. 2019), Alert Management, Photometry and Evaluation of Lightcurves (AMPEL; Nordin et al. 2019), Automatic Learning for the Rapid Classification of Events (ALeRCE; Förster et al. 2020), and Fink (Möller et al. 2021). Alert brokers can filter alerts, add value through annotation from many sources of information, characterize and classify alerts, and distribute alerts to the consumer.

Overall, we view ANTARES as an astronomical instrument, but one that lets scientists collect and analyze time-domain alerts, rather than photons. ANTARES is designed to operate at LSST scale and beyond while ingesting alerts, annotating them with additional information, filtering them, and distributing alerts of interest to astronomers who request them. In this paper, we describe the principles that guided the development, the overall architecture of the system, how the various components work, and the performance as deployed at the ZTF scale. Descriptions of previous versions of the system were presented by Saha et al. (2014, 2016) and Narayan et al. (2018).

2. Illustrative Use Cases

The overarching design goal for ANTARES is to enable the broadest possible scientific use of time-domain alerts generated by large-scale surveys. ANTARES provides a flexible infrastructure that allows the end user to filter and classify alerts in virtually any way that is of interest to them. The scientific aims of ANTARES will be determined largely by the demands and interests of the community that uses it. An exhaustive list of all possible uses is beyond the scope of this paper, but we can describe several use cases that illustrate the requirements for the system. These cases will demonstrate the logic behind the capabilities of ANTARES.

Time-domain surveys with high cadence have enabled detections of transients shortly after they occur. A prime example is SN 2011fe, a Type Ia supernova (SN) in M101, discovered by the Palomar Transient Facility (PTF, the precursor to ZTF; Law et al. 2009) just 11 hours after explosion (Nugent et al. 2011). This rapid identification put constraints on the size of the progenitor, demonstrating that the SN arose from a compact object (Bloom et al. 2012). Other cases of observations soon after explosions of SNe have revealed the nature of nearby circumstellar material and thus the evolutionary state of the progenitor star (e.g., Khazov et al. 2016; de Jaeger et al. 2018; Kochanek 2019; Gangopadhyay et al. 2020; Goldberg et al. 2020; Chugai 2020). In general, astronomers will prefer as complete a picture as possible of the evolution of any transient, so early detection is intrinsically valuable. An effective brokering system will provide early detection and recognition. To do so, it must process time-domain alerts in real time, with latency as low as possible. The LSST alert production system aims to deliver raw alerts within 60 s of the shutter closing (Kantor 2014). In addition, the brokering system must distinguish interesting transients in the alert stream, so it must have a filtering system that uses the alert data, preferably together with any available external sources of information, to automatically flag candidates. The filter could even compare alert data with predicted features from models of objects as yet unobserved.

Identification of some transients benefits greatly from external information. Tidal disruption events (TDEs) can shed light on the nature of black holes, including accretion mechanisms and jet formation (Rees 1988; Metzger & Stone 2016; De Colle & Lu 2020; Hung et al. 2020; Lee et al. 2020a). While the number of discovered TDEs is growing (e.g., Komossa 2015; Hung et al. 2018; van Velzen et al. 2020), the field is still relatively young. TDEs tend to occur in post-starburst galaxies (French et al. 2016, 2017; Cen 2020), although the physical reasons for this are, as yet, unknown. Catalogs of likely TDE hosts exist (French & Zabludoff 2018), so a brokering system can use that knowledge as prior information in a filter for TDE detection. In addition, as TDEs occur at the centers of galaxies, they can be confused with active galactic nuclei (AGNs). A broker can identify AGNs not only through catalogs of known objects, but also from historical detections at radio or X-ray (or other high-energy) wavelengths. A broker must then be flexible in incorporating and updating catalogs of known astronomical objects, especially across the full range of the electromagnetic spectrum to use as much available data as possible in filtering alerts.

As described above, the anticipated number of nightly events that LSST will produce for relatively common transients and variables is quite large (e.g., Ridgway et al. 2014). It may not be necessary to obtain spectroscopic and photometric follow-up of every one of these transients and variables, but given the limited resources (e.g., Kulkarni 2020) and the number of such transients, that scale of follow-up is not even possible. Nonetheless, astronomers will still want to follow and characterize subsets of these objects, perhaps in concert with other observing campaigns. An example could be a program to use Type Ia SNe as cosmological probes (see, e.g., the LSST Dark Energy Science Collaboration Science Road Map[11]). The program may have dedicated spectroscopic resources for only a short time, so a steady stream of Type Ia SNe is only needed for that period. Different groups will have different needs at different times. The broker must be capable of filtering alerts to generate streams of objects and flexible enough to provide these customized streams on demand.

Rare events detected by time-domain surveys will also be of great interest. The recent success in identifying an electromagnetic counterpart to a gravitational wave detection (e.g., Abbott et al. 2017a, 2017b) highlights the scientific value in distinguishing the rare events from the many more common ones that will turn up in the same survey. Many multimessenger events, whether gravitational waves (e.g., LIGO/Virgo, Aasi et al. 2015; Acernese et al. 2015), neutrinos (e.g., Adrián-Martínez et al. 2011; Aartsen et al. 2017), or cosmic rays (e.g., Aharonian et al. 2006; Holder et al. 2006; Knödlseder 2020), have poor sky localizations (e.g., Abbott et al. 2018), necessitating wide-area searches that will produce large numbers of alerts ($\sim$1000 per square degree, at LSST depth) in a short time. It may be possible to use multimessenger data to identify potential host galaxies and restrict the search area (Gehrels et al. 2016), but there will still be a large number of events to sort. In addition, as with other transients, early detection will be valuable (e.g., Arcavi 2018). Even without a multimessenger component, rare events will appear in time-domain surveys. At the LSST rate, there could be several one-in-a-billion events every year. The broker must operate rapidly to filter the alerts and distinguish rare events. One way of finding the needle in the haystack is to remove the hay, so the broker should be able to identify common transients and variables that would otherwise obscure rare events with their numbers. As an example, flares on dwarf stars could be distinguished using multiwavelength data such as checking for

[11] https://doi.org/10.5281/zenodo.3588457

coincidence with red sources in the WISE catalog (e.g., Davenport et al. 2012).

Activity on solar system objects provides another tool for investigating their nature and thus elucidating aspects of solar system formation (e.g., Jewitt et al. 2015). Identification of new moving objects in time-domain surveys employs a distinctly different approach than finding objects that merely change in brightness. It typically requires combining tracks of objects over multiple frames separated by hours to days (e.g., Trilling et al. 2017; Jones et al. 2018). Finding new moving objects is thus beyond the capacity of a broker such as ANTARES, and it is a task that will be a component of LSST data management (Juric et al. 2017). Known solar system objects, however, can be distinguished if the ephemerides are correct. Both ZTF and LSST will flag known objects, and these can then be evaluated to see if they have the expected brightness or if they are showing signs of activity. Such a specialized process on a large subset of a time-domain stream would likely require a separate broker, so a general-purpose broker must be able to efficiently redirect a significant portion of the alert stream to downstream, customized brokers.

Many variable objects do not need immediate spectroscopic or photometric follow-up, especially those with relatively long timescales. These objects, whether periodic or aperiodic, are most valuable to an astronomer once a full light curve is available. Depending on the cadence of the survey and the period of the variable, this may take many periods to sufficiently sample the light curve. To study these objects, real-time filtering is less useful than easy discovery in an archive of alerts. While surveys may retain searchable archives of raw alerts, the broker must keep a record of the full, annotated set of alerts. This value-added archive must be built up by the broker over the course of the survey. It must provide a database of alerts with a flexible query system that enables science on longer timescale objects.

Sometimes variables (and some longer-lived transients) can behave in unexpected ways. Examples could include a known pulsating periodic variable suddenly undergoing an eclipse from a distant companion or an eruption of a luminous blue variable. Wide-field time-domain surveys provide astronomers with a tool that monitors all of these objects. The broker must provide a way for users to provide watch lists of objects of interest and a method of communication to notify these users when an alert occurs for one of their objects.

Finally, as each new time-domain survey has begun, the novel aspects of parameter space that it reaches have inevitably yielded interesting objects that no one had yet detected such as superluminous SNe (e.g., Quimby et al. 2007; Gal-Yam 2012), luminous red novae (e.g., Martini et al. 1999; Kasliwal et al. 2011), calcium-rich transients (e.g., Kasliwal et al. 2012; Foley 2015), .Ia SNe (e.g., Kasliwal et al. 2010; Perets et al. 2010), and fast, blue optical transients (e.g., Drout et al. 2014; Smartt et al. 2018; Margutti et al. 2019). Astronomy has traditionally been a science of discovery and exploration. Wide-field time-domain surveys continue this tradition, providing opportunities for discovery. There are, as yet, still empty regions in the energy–time diagram of Kasliwal (2012). LSST will produce time-domain alerts not only at an unprecedented rate, but also at an unprecedented depth, relatively high cadence, and in multiple filters, thus opening an entirely new discovery volume. We may not know precisely what will appear in the LSST alert stream, but we can predict that new and extraordinary objects will be there. We need to have a broker that can sort through the alerts rapidly, filter them to recognize what we know, and then provide a substream of unusual events that will provide the next breakthrough in astronomy.

3. Data Model

A data model is a set of data entities that exist within a system, the relationships between entities, and the way of representing these entities and relationships in a database. The ANTARES data model is driven by the nature of time-domain data. The primary data entities in ANTARES are the Alert and the Locus. Secondary entities include the Tag, LocusProperty, AlertProperty, WatchList, WatchObject, Catalog, and CatalogObject. The data model is visualized in Figure 1.

An Alert is a message received by ANTARES from a survey such as ZTF or LSST, plus additional properties generated by ANTARES. Typically, an Alert is either an observed magnitude measurement or an “upper limit” magnitude measurement, but in principle, an Alert can be any packet of data that has precise spatial coordinates and a time stamp.[12]

A Locus (plural, Loci) is a point on the sky where Alerts cluster and is roughly equivalent to an astrophysical object. The association of Alerts to Loci uses a 1″ radius cone search. That is, each incoming Alert is associated with the nearest Locus within 1″ of the Alert. If no such Locus exists, a new Locus is created.

Tags are short strings that are associated with one or more Loci. Tags are used to flag loci that meet specific criteria, e.g., “extragalactic,” “nuclear_transient,” etc. Tags are used to generate output streams and are queryable in the database.

Alert properties are associated with a particular Alert, such as magnitude. Some originate from the incoming source alert, and others are annotations generated by Filters.

Locus properties are associated with a Locus (i.e., an astronomical object), not an Alert. Examples include color or statistics of a light curve such as skewness.

CatalogObjects are entities in astronomical object catalogs. ANTARES 1.0 supports extended objects by modeling them as circular regions. Support for other shapes is possible in future versions.

WatchObjects and WatchLists allow users to define and track objects and regions of interest to them. A WatchObject is a coordinate and a radius, and a WatchList is a collection of such objects. Users may create their own WatchLists using the ANTARES Portal (Section 11.1 describes the portal) and browse matching Loci. ANTARES can notify users of new hits to their WatchLists over Slack.[13]

The Provenance object stores information about the version and configuration of ANTARES that processes each Alert. It is described further in Section 8.

[12] Region-based alerts (e.g., gravitational wave detections from LIGO/Virgo) do not have definitive coordinate locations and are handled independently of the Alert/Locus concept. We have implemented a system for ingesting LIGO/Virgo alerts that can be generalized to any alert source with imprecise localizations (and thus large areas associated with the alert), including the neutrino and cosmic-ray observatories mentioned above, and also for networks that collate multimessenger alerts like the Astrophysical Multimessenger Observatory Network (AMON; Ayala Solares et al. 2020). Filters in ANTARES have access to all LIGO/Virgo data within the past 30 days. This makes it possible to write a filter that flags all Alerts within a particular confidence level region of a recent LIGO/Virgo detection. By combining this with other criteria, such as galaxy catalog associations or light-curve history, this allows the production of filters that identify likely LIGO/Virgo correlates.

[13] https://slack.com/

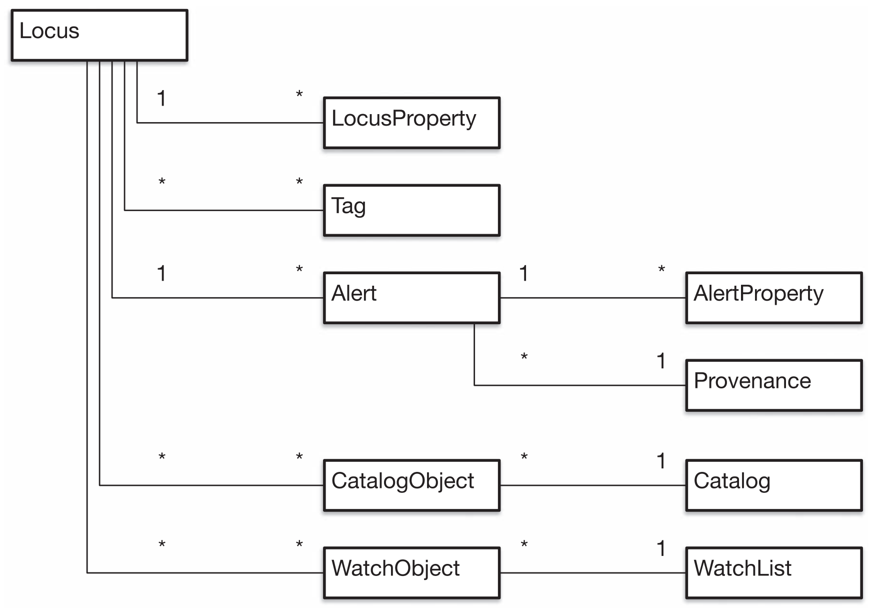

Figure 1. ANTARES data model, simplified. Boxes indicate entities. Lines indicate relationships. Asterisks and numbers on lines indicate relationship type: one to many (1—*), many to one (*—1), or many to many (*—*). Data contained within entities are omitted. The Filter is a software entity, not a data entity, and is also omitted.

4. System Architecture

The ANTARES system is designed around a parallel stream-processing architecture. The system ingests alerts from input Apache Kafka streams (Kafka is an industry-standard technology for data streaming),[14] processes them, stores them in a database, and produces streams of output alerts using Kafka. The system is composed of 10 subsystems that perform specific functions. Figure 2 depicts the layering of systems and activities. Figure 3 depicts the architecture of the system and connections between components. Figure 4 depicts the behavior of the Alert Pipeline subsystem that processes alert streams. The remainder of this section describes these concepts in more detail.

4.1. System Layers

At an abstract level, the system is composed of three layers as shown in Figure 2. From bottom to top, these layers are systems administration, software engineering, and science. Each layer contains responsibilities and systems that facilitate those of the layer above. The systems administration layer is responsible for hosting and managing components that run on bare-metal hardware. This includes the databases, the Kafka streaming message broker, and the Kubernetes[15] (a software container orchestration system) compute cluster. On top of this layer is the software engineering layer, which includes two types of systems, live systems that run on Kubernetes and distributable software packages that users download and run outside the ANTARES cluster. On top of the software engineering layer is the science layer. The science layer consists of tasks and components written by researchers who use ANTARES as a science tool. This includes data analysis tasks, model training, filter development, and downstream processing of ANTARES output streams.

4.2. System Components

We show the architecture of the system in Figure 3. This illustrates the connections between components and the flow of data through the system.

ANTARES processes alerts concurrently in multiple instances of a program called the "Pipeline Worker." We run one instance for each partition in the Kafka topic from which they receive data. Each worker processes alerts in the order they were received and uses Kafka's "commit" mechanism to track progress and remain resilient to system failures. The alerts are processed according to the configured science workload, and the results are stored in the ANTARES database as well as distributed to the community. The Pipeline Workers load Filter code from the MySQL database[16] upon start-up. Loci, Alerts, and their annotations are stored in the Alert Database, which is implemented with Apache Cassandra.[17] The Alert Database is the single source of truth for ANTARES data, although its content is also indexed separately by the Search Engine. The Alert Database schema is designed for fast access by the Pipeline Workers and thus does not support complex queries (see Section 9). The Pipeline Workers perform Locus associations and execute filter code on the Loci (see Section 4.3). After each Locus is processed, updated information about the Locus is sent to the Search Engine (implemented using Elasticsearch[18]) via Kafka and the Index Worker microservice. The Search Engine indexes all Loci and makes them queryable by the Application Programming Interface (API). The API service is a Representational State Transfer (REST) Hypertext Transfer Protocol (HTTP) API that is used by the Portal website and by the Client Library. The API uses the Search Engine to perform searches for Loci, and loads the complete data for each Locus from the Alert Database. The Client Library and the Portal interface with users, providing visibility into the database.

[14] https://kafka.apache.org/
[15] https://kubernetes.io/
[16] https://www.mysql.com/
[17] https://cassandra.apache.org/
[18] https://www.elastic.co/

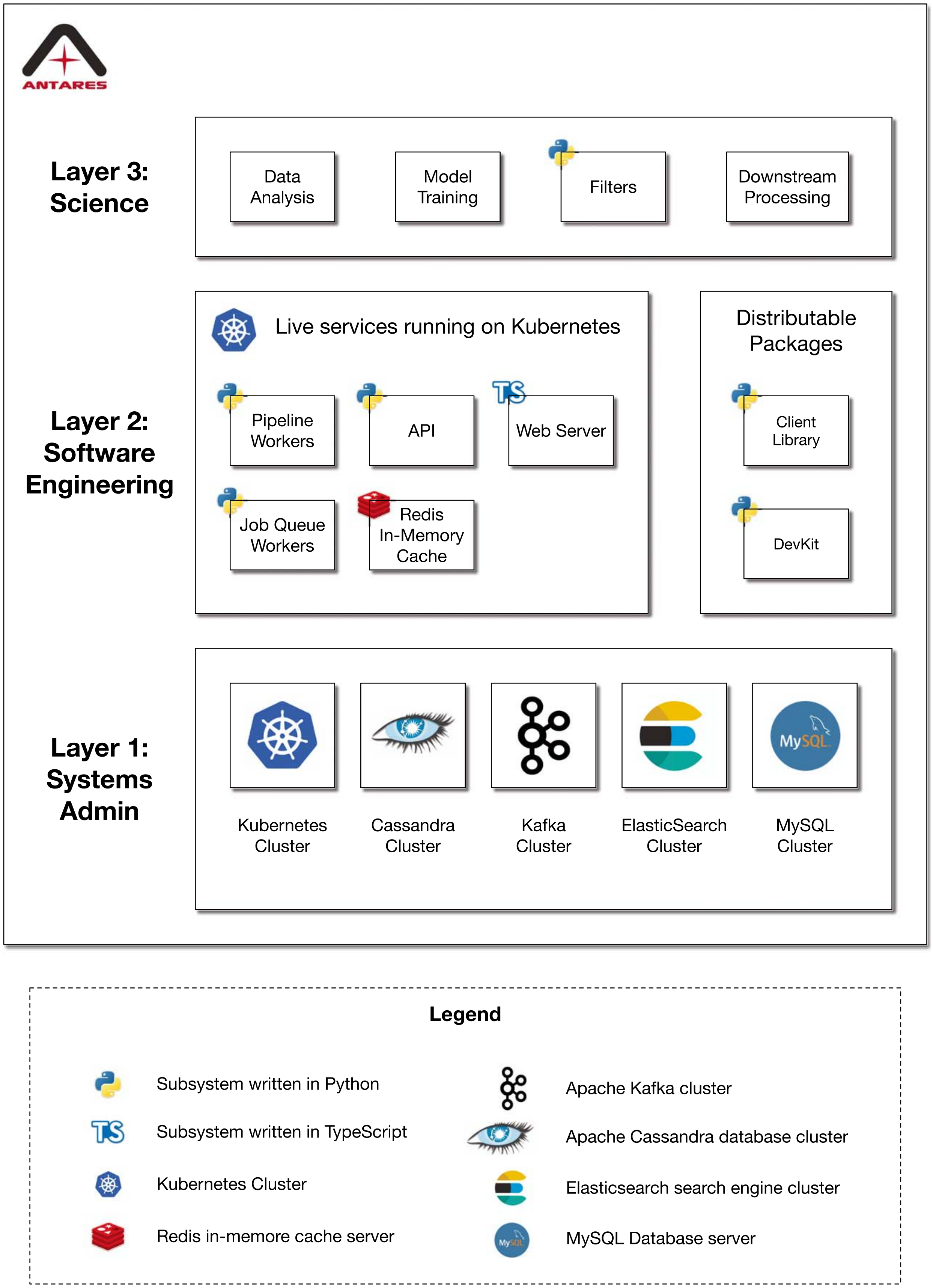

Figure 2. "Layercake" diagram showing the layers of systems and activities in ANTARES. The Systems Administration layer provides compute and database services. The Software Engineering layer provides software systems. The Science layer consists of activities performed by science staff and researchers from the community. This is an abstract representation, not a system architecture diagram.

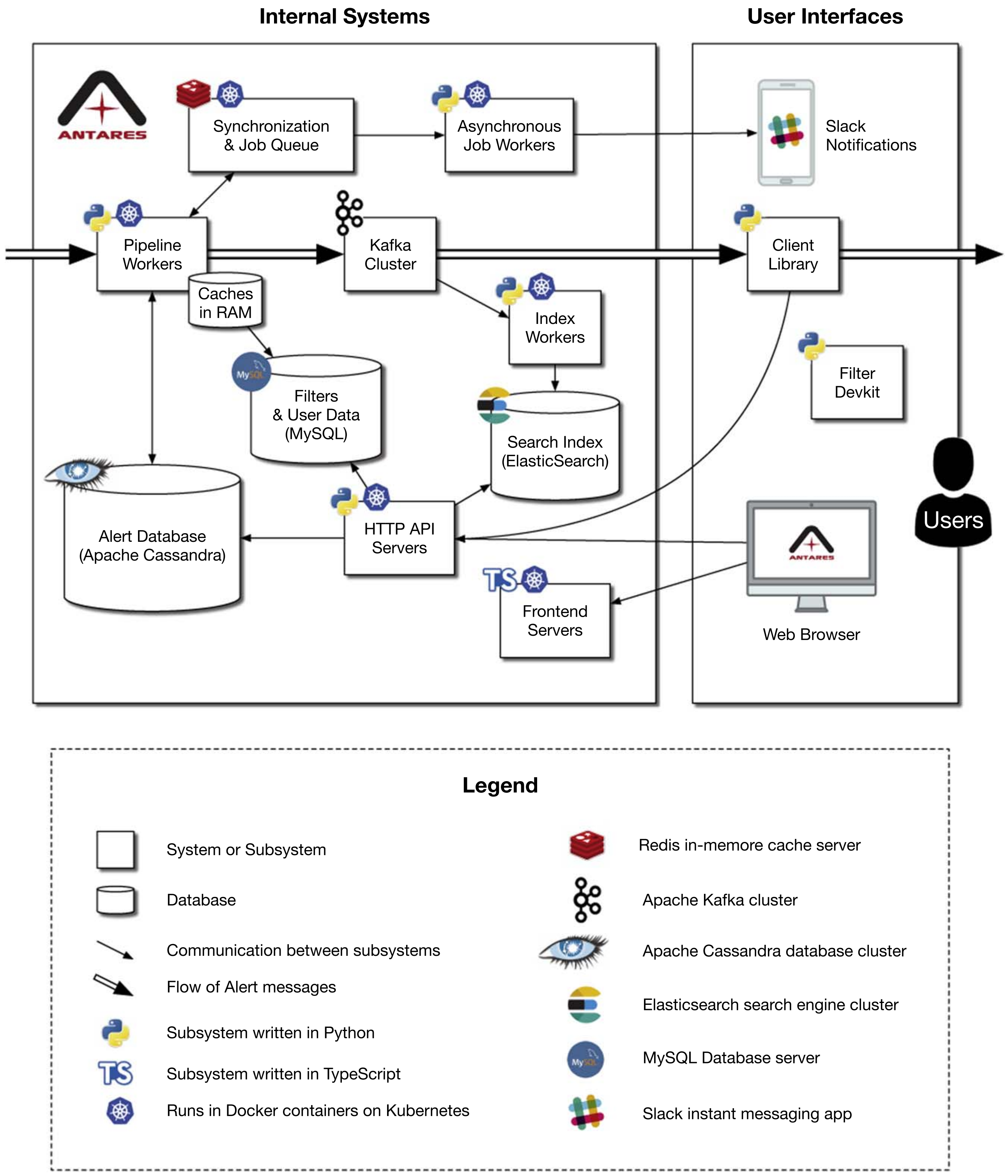
Internal Systems
User Interfaces
ANTARES
Synchronization & Job Queue
Asynchronous Job Workers
Slack Notifications
Pipeline Workers
Kafka Cluster
Client Library
Caches in RAM
Index Workers
Filter Devkit
Filters & User Data (MySQL)
Search Index (ElasticSearch)
Users
Alert Database (Apache Cassandra)
HTTP API Servers
Frontend Servers
Web Browser
Legend
System or Subsystem
Database
Communication between subsystems
Flow of Alert messages
Subsystem written in Python
Subsystem written in TypeScript
Runs in Docker containers on Kubernetes
Redis in-memore cache server
Apache Kafka cluster
Apache Cassandra database cluster
Elasticsearch search engine cluster
MySQL Database server
Slack instant messaging app

Figure 3. Architecture diagram of ANTARES. Input Alerts enter the system on the left (from ZTF, LSST, etc.,) and output Alerts exit on the right (to downstream systems, target and observation managers, etc.,). Many subsystems represent clusters of processes on multiple machines. Subsystems marked with the blue Kubernetes logo run on a shared pool of hardware resources in a Kubernetes cluster. Subsystems not marked with the Kubernetes logo run on dedicated hardware.

The Pipeline Workers also produce two other forms of output, Slack notifications and output Kafka Alerts. Slack messages are sent using an asynchronous cluster of job workers that process tasks in a job queue stored in the Redis[19] in-memory cache system. The workers implement automatic retry and exponential back off in the event that Slack is not responding. This system is designed to facilitate other forms of notification in the future such as web hooks, emails, or Short Message Service (SMS) text messaging as needed. In ANTARES 1.0, only Slack notifications are implemented.

Also shown in the architecture diagram is the Filter Devkit, described in Section 11.3.

[19] https://redis.io/

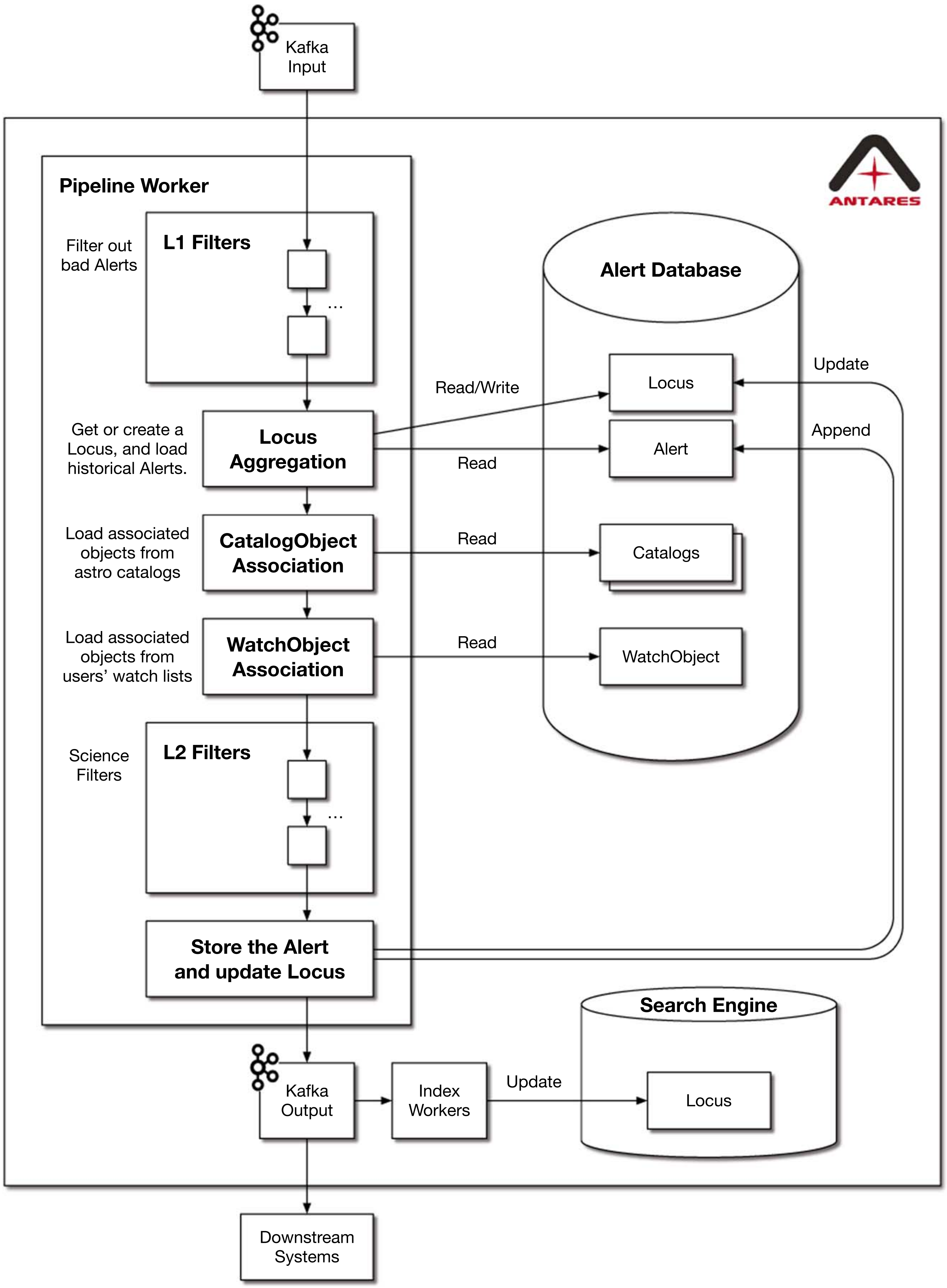

Figure 4. Logical structure of the Alert Pipeline Worker. Input Alert streams are consumed at the top of the diagram and output streams are produced at the bottom.

4.3. Alert Pipeline

The internal structure of the Pipeline Workers is shown in Figure 4. Alerts enter at the top and outputs are produced at the bottom. The first stage of processing is the L1 Filters, which determine whether to run the rest of the pipeline on a given Alert, or whether to simply store it in the database and perform no other processing. This capability can be used to ignore Alerts that are determined to be false detections or of poor quality by some metric. The L1 Filter capability is optional, depending on the ANTARES configuration.

The next step is Locus Aggregation, in which the incoming Alert is assigned to a Locus object. This process uses a 1″ radius cone search. That is, each incoming Alert is associated with the nearest Locus within 1″ of the Alert, with precedence given to survey-provided associations. If no such Locus exists, a new Locus is created there and is assigned a unique "locus_id." If there is a preexisting Locus, then all historical Alerts associated with it are loaded from the database. From this point onward in the pipeline, the object being processed is a Locus object, not an Alert object.

The next stages of our pipeline are CatalogObject Association and WatchObject Association, in which CatalogObjects and WatchObjects are loaded for the given Locus. This is the first step in annotating the Locus with value-added data. This is described in detail in Section 5.

With all known data loaded for the Locus, the pipeline executes the L2 Filters or "Science Filters." These are Filters developed by the ANTARES science staff (e.g., Soraisam et al. 2020) or submitted by the community. Filters are described in Section 6. They implement science use cases such as classification and other decision-making.

Finally, the new Alert is written to the database and the Locus is updated with whatever new properties and associations it has acquired. Output Alerts are broadcast to downstream systems using Kafka, and the Search Engine is updated with the new Locus information.

4.4. Fault Tolerance

ANTARES runs the Filter code submitted by the community, which is difficult to rigorously test. Therefore, ANTARES expects and handles filter crashes. Filters are immediately disabled if they crash, and a notification is sent to the author via Slack. The notification contains a "crash_log_id" and the "locus_id" of the Locus that was being processed, allowing the author to inspect the error and replicate the fault using the Devkit (see Section 11.3). The author may then improve the Filter, test it on actual data, and submit a new version. Other than the temporary downtime of the Filter, there are no negative consequences to this occurring. From experience, we have found that this capability is essential when developing new Filters.

Every component in the main ANTARES data pathway is a distributed system, allowing continuous operations in the event of a hardware failure of one machine at a time. The simultaneous failure of multiple machines may require a hands-on systems administration response.

ANTARES' fault tolerance capabilities benefit from the properties of Kubernetes and Kafka. Specifically, Alerts that are received are not "committed" (i.e., marked as received) in Kafka until their processing is complete. Therefore, when a Pipeline Worker crashes in an unexpected way, it can pick up where it left off when it reboots. Kubernetes automatically restarts containers that fail.

Each system in the main data pathway is idempotent. This means that if the same Alert is received more than once, the final data in the Alert is correct. For example, duplicate Alerts are detected and skipped.

5. Annotation

In addition to the base data included in the original alert, ANTARES attaches data and associations to Alerts and Loci. We call these "value-added" data Annotations. Annotations have three purposes: to provide richer input data for Filters, to allow Filters to store computed properties on Loci and Alerts, and to allow searchability of the database by meaningful criteria. ANTARES includes several types of annotations, including Locus properties, Alert properties, Locus Tags, astronomical catalog object associations, and associations with watched objects.

Catalog associations are performed by first modeling each catalog object as circular regions of the sky of a particular radius. Each Locus is annotated with all catalog objects whose circular region the Locus falls within. In the case of extended objects, the radius of each object region is taken from the catalog data. In the case of point sources, the object is given a default value of 1″.

The catalog search algorithm uses a hierarchical triangular mesh (HTM; Kunszt et al. 2001) ID lookup-table (HTMLUT). The HTMLUT allows for efficient and scalable object associations. Each catalog object is entered into the HTMLUT multiple times, once for each HTM trixel ID that the catalog object's circular region intersects. Because HTM trixel regions are triangular and not circular, the region for each object in the HTMLUT is larger than the circular region representing the catalog object. Therefore, false-positive associations occur when using HTMLUT alone. To resolve this, the position and radius of each object are checked after loading their data, and false positives are removed.

The HTMLUT is multilevel, meaning that it supports HTM IDs at multiple levels of tessellation. Each catalog object is represented at a level of tessellation calculated from its radius. The algorithm is tuned to select an HTM tessellation level such that each object intersects 2.5 HTM trixels on average. This level provides an approximate balance between minimizing the number of entries in the HTMLUT and minimizing the number of false positives that have to be loaded, checked, and removed.

The HTMLUT scheme can represent object regions of any size and shape, given an algorithm to represent the region as a set of HTM trixels at various tessellation levels. In ANTARES 1.0, circular regions have been implemented. Ellipses or other shapes can be implemented in the future.

The exact complement of catalogs will evolve as new catalogs are made available or old ones are updated, but LSST data will be incorporated as catalogs are published. The current set of catalogs in ANTARES is listed in Table 1, many derived from catsHTM (Soumagnac & Ofek 2018). Several catalogs in ANTARES 1.0 make use of variable radii, including the Third Reference Catalogue of Bright Galaxies (RC3), the Revised Catalog of GALEX Ultraviolet Sources (GALEX), and The Two Micron All Sky Survey (2MASS) extended source catalogs. In the case of RC3, we adopted a search radius associated with the apparent major isophotal diameter. We are using D25, measured at the surface brightness level $\mu_B = 25.0$ B-mag per square arcsecond. For GALEX, we adopted a search

Table 1
External Catalogs used in ANTARES

Catalog	Reference
The Two Micron All Sky Survey	Skrutskie et al. (2006)
AllWISE Data Release	Cutri et al. (2014)
ASAS-SN Catalog of Variable Stars	Shappee et al. (2014); Jayasinghe et al. (2018, 2019a, 2019b)
Second-Generation Guide Star Catalog	Lasker et al. (2008)
Chandra Source Catalog	Evans et al. (2010)
Catalina Surveys	Drake et al. (2013a, 2013b, 2014), Torrealba et al. (2015), Drake et al. (2017)
Preferred Tidal Disruption Hosts	French & Zabludoff (2018)
Gaia Data Release 2	Gaia Collaboration et al. (2018)
The NASA/IPAC Extragalactic Database[a]	Helou et al. (1995)
New York University Value-Added Galaxy Catalog	Blanton et al. (2005)
Third Reference Catalogue of Bright Galaxies	de Vaucouleurs et al. (1991); Corwin et al. (1994)
Sloan Digital Sky Survey Data Release 12	Alam et al. (2015)
A Catalogue of Quasars and Active Nuclei: 13th Edition	Véron-Cetty & Véron (2010)
The Third XMM-Newton Serendipitous Source Catalogue	Rosen et al. (2016)
Revised Catalog of GALEX Ultraviolet Sources	Bianchi et al. (2017)

Note.
[a] The NASA/IPAC Extragalactic Database (NED) is funded by the National Aeronautics and Space Administration and operated by the California Institute of Technology.

radius associated with the Kron radius in the NUV. In practice, the Kron radius is expressed in the form of NUV_KRON_RADIUS * NUV_A_WORLD in the GALEX catalog (Bianchi et al. 2017). We thus adopt this form to define our search radius for GALEX. For the 2MASS extended source catalog, we use the semimajor axis (in arcseconds) of a fiducial ellipse at isophote $K = 20$ mag arcsec^{-2}, taken from the catalog data field "r_k20fe."

Catalogs used by ANTARES are stored locally within the Cassandra database. This allows our HTMLUT system to be used and eliminates the latency and reliability issues associated with querying to external databases hundreds of times per second.

6. Filters

The Filter is the primary way in which users of ANTARES can winnow a stream of time-domain alerts. By evaluating data, both from the alert and annotations, algorithms implemented in filters can identify objects of interest and eliminate irrelevant objects, producing a subset of alerts that astronomers can then pursue with other observational resources. ANTARES Filters are snippets of Python (Van Rossum & Drake 2009) code that process incoming Alerts. Filters can be built into the ANTARES codebase or can be submitted by the community using the ANTARES web Portal. Filters are executed in a sequence called the Filter Pipeline (see Figure 4). The Pipeline runs on each Locus when a new Alert is received on that Locus. Filters can use data files such as statistical models, neural networks, lookup tables, etc. These repositories represent distillations of astronomical knowledge derived from larger samples (e.g., Soraisam et al. 2020). These larger samples are what we call a Touchstone for ANTARES, but the Touchstone itself is external to the Pipeline described here. It is a separate system that enables the design, training, and deployment of filters.

6.1. Filter Inputs and Outputs

Filters have access to a variety of information sources in ANTARES at runtime, including the Locus object and its properties and Tags, all catalog objects associated with the Locus, all Alerts associated with the Locus and their properties, and recent LIGO/Virgo detection reports. Time-series data such as Alert properties over time are available as "Astropy.TimeSeries" objects (Astropy Collaboration et al. 2013) or as Pandas dataframes (McKinney 2010). Other data are represented as Python data structures.

Based on the input data, Filters may take several actions, including setting properties on the Locus, setting properties on the newly arrived Alert (but not on historical Alerts), adding Tags to the Locus, or halting the pipeline and thus preventing subsequent Filters from running. This last ability is restricted to prevent misuse. Properties may be of type float64, string, or long integer.

6.2. Filter Structure

Filters are Python classes that inherit from class "antares.devkit.Filter" and implement, at minimum, a method `run (self, locus)`. A simple filter is the HelloWorld filter, shown below. The HelloWorld filter declares that it may produce a Tag called "hello_world" and gives the Tag a text description. Then, in the `run` method, the filter adds the tag to the locus. There is no conditional logic around adding the tag, so this tag will be added to every locus that the Filter sees.

```
import antares.devkit as dk
class HelloWorld(dk.Filter):
OUTPUT_TAGS = [
{
'name': 'hello_world',
'description': 'This tag is added to EVERY Locus.',
},
]
def run(self, locus):
locus.tag('hello_world')
```

The HelloWorld filter is a trivial example to demonstrate the basic format of a filter. Appendix contains a more complex, real-world example. There, we present a high signal-to-noise ratio filter that explicitly declares all inputs and outputs, performs initial setup, executes a simple computation, conditionally adds a Tag depending on input data, and handles a potential error case.

7. Outputs

The output of ANTARES takes three forms. These are our searchable database, Slack notifications through our Slack workspace,[20] and Kafka streams. The database is searchable using the ANTARES Portal and can also be queried using the HTTP API either by users or by autonomous systems. Slack notifications are used to inform users and teams of events in real time. This includes newly tagged Loci, new Alerts on tagged Loci, and hits to WatchLists. ANTARES output Kafka streams are intended to be consumed by downstream systems. Streams are produced by tagging Loci. Each stream is configurable to include a union or intersection of one or more Tags. For example, given a Filter that tags some Loci "extragalactic" and another Filter that tags some Loci "sn1a_candidate," a stream could be configured to include all Alerts whose Loci have both tags. A system could then connect to that stream and receive all such alerts from ANTARES. Connections to the HTTP API and Kafka streams are facilitated by the ANTARES Client Library, discussed in Section 11.2.

8. Provenance Tracking

We considered two primary use cases for tracking provenance data associated with the processing of alerts by ANTARES: first, reproducing offline the state of the ANTARES system at a time in the past, and, second, viewing how filter decision-making changed over time on a Locus. An example of the first use case would be if an astronomer wished to inspect an Alert that was processed by ANTARES in the past. This individual could, based on the provenance data, run a copy of ANTARES with the same configuration as ran in production and reproduce the decisions made while evaluating that alert. As an example of the second use case, given a Filter that produces a classification prediction, a user might wish to view how their Filter's classification of a given Locus changed as each new Alert was received and processed.

To address the first use case, ANTARES logs all of its configuration and state on start-up. When each ANTARES process boots up, it records information about the version of the system, the version of all dependencies, catalogs, filters, etc. The full content of the Provenance Log is shown in Table 2. This information is stored as a Provenance Log object in the database, indexed by a provenance_id. Each incoming Alert is annotated with the provenance_id of the ANTARES process that received it. Thus, the state of the system that processed a given Alert can be retrieved and, if necessary, reproduced offline. To simplify the state of ANTARES, the system does not add/remove Filters while running. Instead, the system reboots automatically every 24 hr and updates its filter set and configuration at that time only. If necessary, the system can be manually rebooted more frequently with no negative effect on operations.

To address the second provenance use case, ANTARES allows Filters to record time-series of variables. This is implemented using Alert properties. Alert properties can be written to the current (i.e., new) Alert under consideration by a Filter and are immutable thereafter. For example, a Filter could exist that predicts the probability that a Locus is an RR Lyrae variable star. Each time the Filter runs, it could store that probability as an Alert property on the new Alert. Then, the Filter's author can view this value over time using the Client library or the Devkit.

[20] https://antares-noao.slack.com

Table 2
ANTARES Provenance Log Content

Provenance Label	Description
antares_version	ANTARES package version
config	ANTARES system configuration
filters	Active Filters with version numbers
catalogs	Active Catalogs
python_packages	Python package versions

9. Database Design

The data model described above is implemented using two databases, the alert database and the search index. These databases are implemented using Cassandra and Elasticsearch, respectively. Cassandra stores all data in a high-performance and scalable manner, but is indexed only by Locus ID and sky coordinate (represented by HTM IDs). Elasticsearch provides search indexes over values such as Locus properties, Tags, and catalog matches. To reduce capacity requirements, Elasticsearch stores only Locus data, not Alert data.

9.1. Apache Cassandra—ANTARES Alert Database

Cassandra was chosen for its horizontal scalability and performance. The final size of the ANTARES data set is estimated at between 100 TB and 2 PB. The estimate varies depending on many factors such as the final specification of the LSST alert packet contents, and the number of annotations that Filters produce. Taking the upper limit of 2 PB, Cassandra handles volumes of this size in many organizations. Apple famously operates the largest publicly known cluster that, as of 2015, stored 10 PB of data on 75,000 nodes.[21] Cassandra supports the Apache Spark[22] distributed cluster-computing framework, which opens the possibility of developing batch-processing jobs to run over the entire ANTARES data set in the future. ANTARES uses a Cassandra replication factor of 3 to ensure durability of data.

ANTARES uses custom tooling to monitor and operate our Cassandra cluster, which contains six nodes at the time of the ANTARES 1.0 release. These tools report real-time performance and status metrics, gather logs and monitor the health of the cluster, and send Slack notifications in the event of problems. The tools also allow the scheduling and triggering of Cassandra's built-in anti-entropy repair feature that we run weekly. Another custom tool, called "my2cass," allows object catalogs stored in MySQL to be automatically migrated into Cassandra. This entails inspecting the MySQL table schema, creating an equivalent table in Cassandra, copying data into Cassandra using the ANTARES distributed job queue system, and populating the HTMLUT. These investments in operational capability are essential, as the Cassandra cluster will grow significantly over the 10 yr of LSST operations.

9.2. Elasticsearch—ANTARES Search Engine

Our Cassandra database is designed to handle the particular set of queries described in 4.4. This allows it to handle

[21] https://cassandra.apache.org/
[22] https://dl.acm.org/doi/10.1145/2934664

LSST-scale throughput but prevents users from writing more complex queries to search for data they want. In order to allow for flexible searches over the ANTARES data holdings, we additionally store information about all of the Loci we have processed in an Elasticsearch cluster. Elasticsearch is a search engine built around Apache Lucene that allows our team and users to find Loci and compute aggregate statistics. It was chosen for its efficient addition of new indexes to existing tables, and horizontal scalability. Because new Locus properties, Tags, and Catalogs will be added continuously over time, the Search Engine needs to be able to efficiently add new indexes. ANTARES automatically creates appropriately typed indexes in Elasticsearch as this occurs. At the ZTF scale, a single-node Elasticsearch cluster suffices to store the search index. At the LSST scale, the Elasticsearch will need to be expanded out to multiple nodes.

10. Performance

Over the 10 yr of LSST operations, the lengths of the light curves of variable objects will increase linearly from zero to hundreds of data points per Locus. Because ANTARES allows Filters to process the complete Locus history data each time an Alert is received, the load on the system will increase linearly over time. This is true both in computational load and read load on the database. Experience with pre-Cassandra designs of ANTARES running on ZTF data has taught us to plan ahead. In the first few months of ZTF data, a single MySQL node could easily act as the Alert Database. After more than a year of ZTF data, this was untenable. A distributed database was required. This linearly increasing load demands that long-term scaling plans be made in advance. No static system configuration that works at year 1 is guaranteed to work at year 10, or even at year 3.

Alert streams have the useful property that each Alert can be processed independently of other nearby Alerts, as long as they are not close enough together that they may belong to the same object (1″). ANTARES makes use of this property by processing data in parallel. The default configuration in our load tests has been 10 ANTARES processes, each with 10 threads. The number of processes and threads per process can be increased at any time, given sufficient hardware. Likewise, the database needs to scale over time. This is a matter of both capacity and performance. Response times must be low enough that ANTARES keeps up with the incoming data.

There is one barrier to arbitrarily scaling the system that can be addressed when needed. Kafka topics from ZTF (and from LSST) are internally split into multiple partitions. Kafka distributes messages approximately evenly between partitions. Kafka topic partitions allow a consumer (technically, a "consumer group") to pull messages from a Kafka topic using multiple processes simultaneously. The number of processes can only be as large as the number of partitions. If, in the future, this becomes a bottleneck, ANTARES may simply repartition the Kafka stream into more partitions by mirroring it into a local Kafka cluster with more partitions.

Although alert processing occurs in parallel, there are two process coordination tasks that occur at the beginning of the processing of each alert. First, a mutex-like[23] locking mechanism prevents two Alerts on the same Locus from being processed at the same time. This mechanism is called the HTM Region Lock. Implemented using Redis and Lua[24] scripts, the region lock allows processes to lock access to sets of HTM trixels in an atomic, thread-safe manner. This is a bottleneck. However, the load on this system is constant over time and does not increase as light curves lengthen. In testing, the region lock introduces 10–100 ms of latency into the pipeline when processing Alerts at a test rate of 10 alerts s^{-1}. This small latency cost is acceptable to prevent race conditions. If this latency grows to unacceptable levels at LSST alert rates, then we will spread the load over multiple Redis instances.

Second, in the event of creating a new Locus object, a unique "locus_id" is generated using a counter stored in memory in Redis. Earlier ANTARES designs used random GUIDs such as "1c165092-a540-11ea-94be-324c811e1e2." By using an integer counter and converting the integer to a compressed string format, Locus IDs can instead take a human-readable form such as "ANT2020so7ia." This system was inspired by the ZTF Object ID scheme, (e.g., "ZTF18aabejqj") and produces shorter, more recognizable identifiers than UUIDs. As with the HTM Region Lock, the performance is acceptable. The system recovers gracefully from Redis failures.

10.1. Scalability Properties

We conjecture that ANTARES scales in proportion to three variables: the rate of incoming alerts, R; the number of historical alerts stored in the database, N (the integral of R over time); and the total computational complexity of filters, F. Note that N is somewhat related to the average length of all light curves in the database, which grows over time as the survey operates. We further conjecture that the number of worker processes and the number of Cassandra database nodes both must scale in proportion to a function of R and N, while the CPU usage of the system scales in proportion to a function of all three variables R, N, and F.

Note that the value of N increases linearly with time as it integrates R. Therefore, even with constant R, the load on ANTARES increases over time.

An estimate of the alert rate, R, can be made based on LSST's estimated value of 10 million alerts per night and a typical night lasting 10 hr. This gives an average alert rate of about 280 alerts per second over the course of the night. Over shorter time intervals, the rate will vary greatly over the course of a night, with spikes of much higher rates. Because alerts are queued and buffered in Kafka, ANTARES does not need to meet the maximum spike throughput rate, but it does need to easily handle the average rate over the course of each night.

10.2. ZTF-scale Load Test Results

We present the results of a load test of ANTARES using 1.23 million alerts taken from eight consecutive nights of ZTF data. The alerts were loaded into a single Kafka topic (stream) with 20 partitions on a Kafka cluster of 10 nodes running on a cloud service provider. ANTARES was deployed on site at NOIRLab and was configured to connect to this stream with 20 worker processes. Each process had 10 threads for a total of 200 threads. The system under test was the ANTARES infrastructure and database, not a particular combination of filters. A single filter was enabled with an average execution

[23] A mutex, or mutual exclusion object, allows multiple program threads to share the same resource, but not to use the resource simultaneously.

[24] http://www.lua.org/

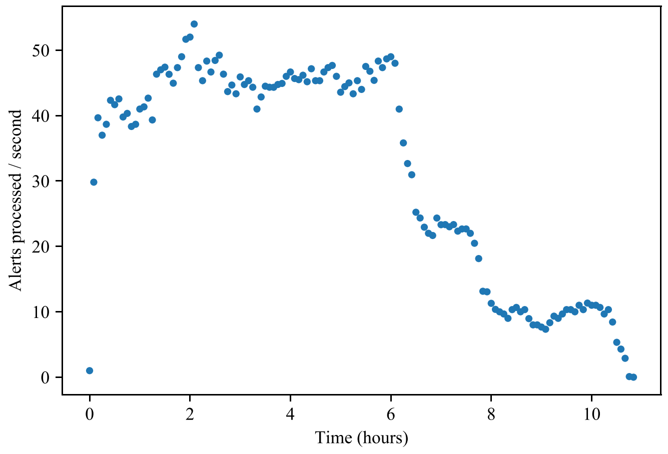

Figure 5. Alert throughput over time as ANTARES processes 1.23 million ZTF alerts in approximately 11 hr. The data set was created by merging eight consecutive nights of ZTF data into a single input stream for ANTARES.

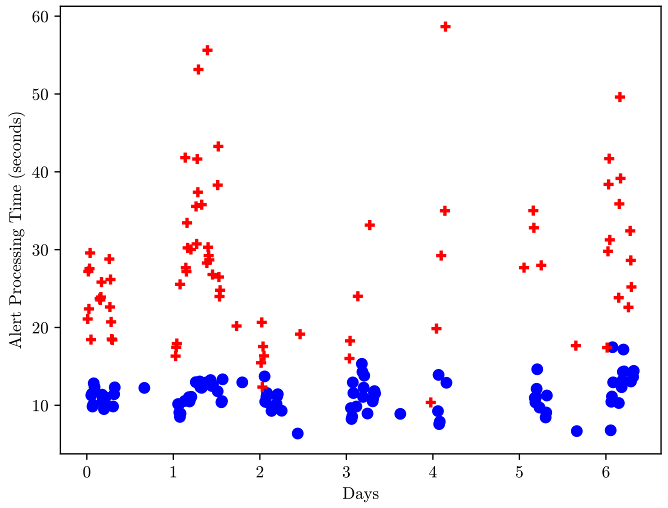

Figure 6. Data from several days of operation showing the time that an alert spends in the ANTARES pipeline. Blue dots represent median values while red crosses show the maximum time spent in the pipeline for each of the operating windows plotted.

time of less than 1 ms. Alert processing rate over time is shown in Figure 5. A steady-state throughput rate of approximately 45 alerts s^{-1} is visible for the first 6 hr. The rate then drops stepwise until all alerts have finished being processed at approximately $t = 11$ hr.

The stepwise decrease in throughput rate toward the end of the processing run has been observed during multiple tests and appears to be scale-invariant with respect to the number of alerts in the run. We conjecture that this phenomenon is an artifact of Apache Kafka. Kafka divides each stream into multiple parallel substreams called partitions. A group of processes that together consume a single topic is called a "consumer group." Each individual consumer process in the consumer group may consume from multiple partitions, but each partition may only be consumed by one consumer process at a time. Some partitions finish being processed before others, and their consumers then sit idle while the slower partitions finish. We suspect that this causes a "tail" effect on plots of throughput over time and is consistent with the stepwise nature of the tail toward the end of a processing run. We will continue to investigate this.

We have observed that steady-state throughput rate of ANTARES is dependent on which Kafka input cluster is used and on the number of partitions in the topic. We measure CPU, memory, and local network well below full utilization. This leads us to speculate that ANTARES' capability with current hardware is limited by the input stream rather than by the database, local network, or CPU and memory constraints. This may be due to the internet connection to the Kafka cluster, to the number of nodes in the Kafka cluster, or to the number of partitions in the topic. We will investigate this further by using a local Kafka cluster directly connected to the ANTARES local network and by varying the number of nodes and the number of partitions.

10.3. Alert Processing Time

Figure 6 shows the typical times that ANTARES takes to process alerts. We define this as the time that an alert spends in the ANTARES pipeline from beginning to end. These data were taken from 7 days of real-time processing of ZTF alerts. Because ANTARES is multiprocess and multithreaded, many alerts are in some stage of the pipeline at any given moment. The total throughput has been tested at 45 alerts s^{-1} as described above, but each alert spends multiple seconds in the pipeline. In Figure 6, we show that the median alert processing time is around 11 s and the maximum is typically between 30 and 60 s.

10.4. Opportunities for Performance Increases

As discussed above, every subsystem of ANTARES is scalable including the Cassandra database and the Alert Pipeline. LSST throughput rates will be about 10x higher than the test result presented above. Also, LSST operations will demand continuous scaling over time because the size of the alert database will grow linearly. We expect to achieve the required scale by expanding the ANTARES server clusters. In addition to simply adding servers, we will continue to pursue performance improvements to the system. Cassandra is highly tunable, and we will continue to investigate how best to configure it for our particular query paths.

In the event that technology or funding limits our ability to scale the system, we have contingency options. One option is to use Level 1 Filters more aggressively to filter out artifacts and other nonastrophysical alerts. Another is to discard the majority of input alert properties and keep only an essential subset. Depending on the content of the LSST alert packet, this could significantly decrease our database capacity needs while preserving our science use cases. Another option is to store all data but only process a subset of Loci in real time according to some filtering. Other data could be stored and deferred for daytime processing (although the day only adds a factor of 2, as night will fall again). We consider these options to be undesirable, and we do not plan to implement them. We expect to achieve the required scale by adding nodes and by tuning Cassandra and the ANTARES pipeline.

11. User Interface

The ANTARES user interface has three components: the Web Portal, the API and companion Client library, and the Filter Devkit.

11.1. Web Portal

The "Portal" is a client-side web application that lets scientists submit filters and visually explore our database. The homepage (https://antares.noirlab.edu/) shows the most recent data that the

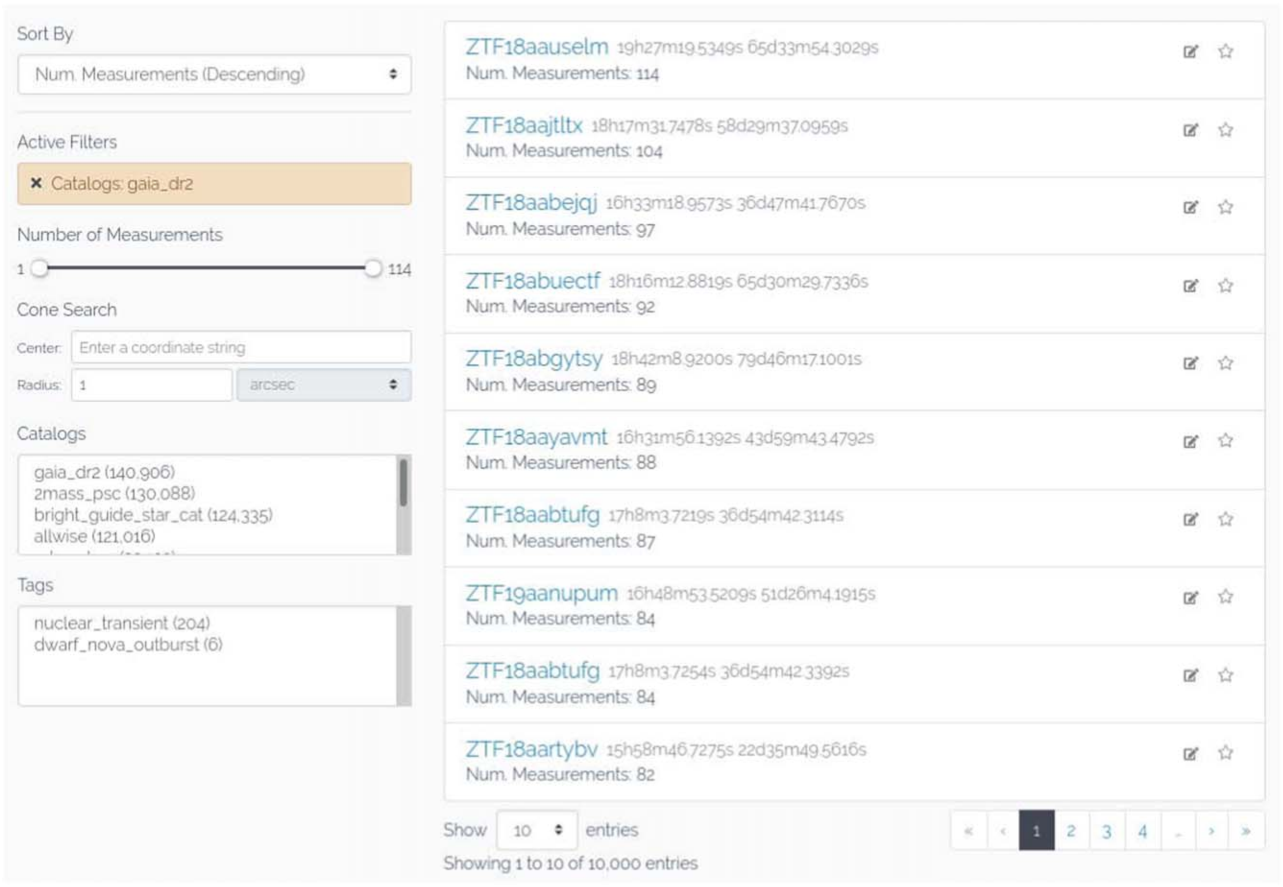

Sort By: Num. Measurements (Descending)

Active Filters: × Catalogs: gaia_dr2

Number of Measurements: 1 – 114

Cone Search
Center: Enter a coordinate string
Radius: 1 arcsec

Catalogs
gaia_dr2 (140,906)
2mass_psc (130,088)
bright_guide_star_cat (124,335)
allwise (121,016)

Tags
nuclear_transient (204)
dwarf_nova_outburst (6)

ZTF18aauselm 19h27m19.5349s 65d33m54.3029s
Num. Measurements: 114

ZTF18aajtltx 18h17m31.7478s 58d29m37.0959s
Num. Measurements: 104

ZTF18aabejqj 16h33m18.9573s 36d47m41.7670s
Num. Measurements: 97

ZTF18abuectf 18h16m12.8819s 65d30m29.7336s
Num. Measurements: 92

ZTF18abgytsy 18h42m8.9200s 79d46m17.1001s
Num. Measurements: 89

ZTF18aayavmt 16h31m56.1392s 43d59m43.4792s
Num. Measurements: 88

ZTF18aabtufg 17h8m3.7219s 36d54m42.3114s
Num. Measurements: 87

ZTF19aanupum 16h48m53.5209s 51d26m4.1915s
Num. Measurements: 84

ZTF18aabtufg 17h8m3.7254s 36d54m42.3392s
Num. Measurements: 84

ZTF18aartybv 15h58m46.7275s 22d35m49.5616s
Num. Measurements: 82

Show 10 entries « ‹ 1 2 3 4 … › »

Showing 1 to 10 of 10,000 entries

Figure 7. Web-based search interface for the ANTARES Portal. Users can interactively refine search result sets along a number of different dimensions, including properties of the object (its location and the number of measurements there), catalog associations, and annotations added to the locus by filters (tags). Users are also able to bookmark and make private annotations on loci.

system has processed, aggregate statistics about the ANTARES data holdings (see Figure 7), and details about particular loci (see Figure 8). Because manually constructing Elasticsearch queries (for the locus search engine) is difficult, we allow users to interactively build search queries for loci that meet certain criteria and then to export them for use in the ANTARES client (see Section 11.2). The Portal also provides an administrative interface for submitting, approving, and managing filters and watch lists in the pipeline.

11.2. Application Programming Interface and Client Library

ANTARES allows for interactive and programmatic data access through an HTTP API. This API exposes "resources," views into our database that generally align with the data models described in Section 3. For example, the request `GET /loci` will receive as response a collection of "locus" resources that each have a light curve, a set of locus properties, etc. We chose to build the API in accordance with version 1.0 of the JavaScript Object Notation:API (JSON:API) specification.[25] This decision was motivated by a number of considerations. A JSON:API supports partial fetching of resources (e.g., fetch just the light curve of a locus) and the ability to include related resources in a request (e.g., fetch a locus and its most recent alert). It also allows for hypermedia-driven interactions that improve discoverability of our data and simplify maintaining backwards compatibility as we continue development work. In short, it allowed us to build an API that supports a rich range of queries, minimizes network traffic, and leverages tools from an existing ecosystem of software for producing and consuming JSON:API-conformant data.

We also provide a user-friendly Python library, the "ANTARES Client," that supports scientists in consuming streaming data through Kafka streams and in analyses of the ANTARES data holdings through the HTTP API. It also includes a command-line interface that enables common tasks such as running a daemon to save a local copy of all the data from a particular stream. A copy of this client library is hosted on the Python Package Index[26] so it can be installed with the Python package manager "pip." Currently, the interfaces provided in the client access resources through the API, which does not require the user to be authenticated. We plan to expand these in the future so that users can programmatically access data such as objects of interest that they have bookmarked. Consuming data from Kafka streams requires credentials that the ANTARES team provides upon request. Documentation for installing and using the client library is provided as a standalone website.[27]

The Client library was used to discover the first R Coronae Borealis star from the ZTF public survey (Lee et al. 2020b). Candidates were preselected using color–color cuts, and their long-term light curves were loaded from the alert database.

[25] https://jsonapi.org/format/1.0/

[26] https://pypi.org/project/antares-client/

[27] https://noao.gitlab.io/antares/client/

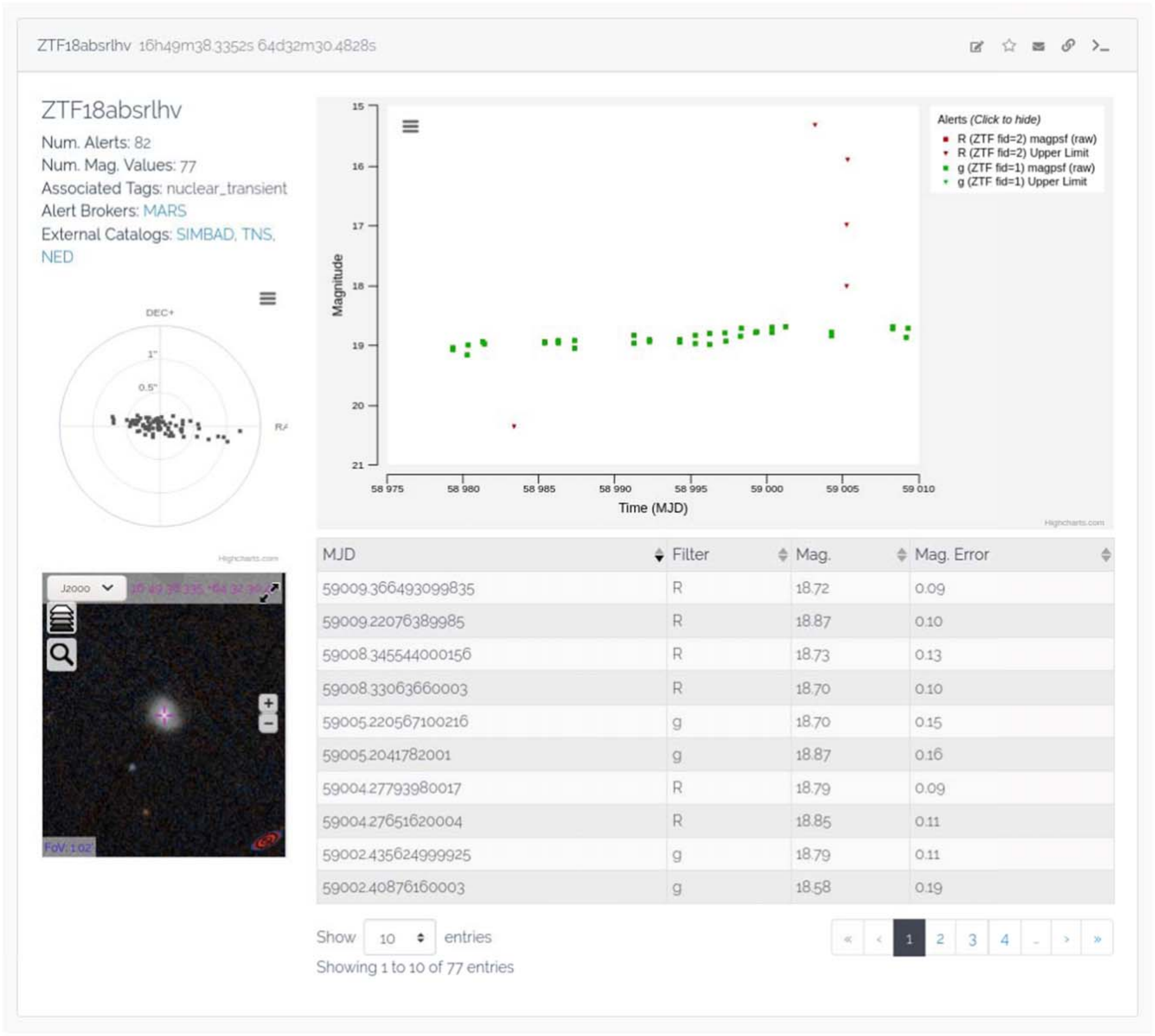
ZTF18absrlhv 16h49m38.3352s 64d32m30.4828s
Magnitude
Time (MJD)
Alerts (Click to hide)
R (ZTF fid=2) magpsf (raw)
R (ZTF fid=2) Upper Limit
g (ZTF fid=1) magpsf (raw)
g (ZTF fid=1) Upper Limit
DEC+
RA
1"
0.5"
J2000
FoV: 1.02'
Highcharts.com

ZTF18absrlhv

Num. Alerts: 82
Num. Mag. Values: 77
Associated Tags: nuclear_transient
Alert Brokers: MARS
External Catalogs: SIMBAD, TNS, NED

MJD	Filter	Mag.	Mag. Error
59009.366493099835	R	18.72	0.09
59009.22076389985	R	18.87	0.10
59008.345544000156	R	18.73	0.13
59008.33063660003	R	18.70	0.10
59005.220567100216	g	18.70	0.15
59005.2041782001	g	18.87	0.16
59004.27793980017	R	18.79	0.09
59004.27651620004	R	18.85	0.11
59002.435624999925	g	18.79	0.11
59002.40876160003	g	18.58	0.19

Show 10 entries
Showing 1 to 10 of 77 entries

« ‹ 1 2 3 4 … › »

Figure 8. Viewing the details of a locus on the ANTARES Portal. Users can see a plot of the light curve of the object, a table of observed values, links to external catalogs, the positions of detections relative to the locus center, and a thumbnail view of the region powered by Aladdin Lite (Bonnarel et al. 2000; Boch & Fernique 2014).

Upon further inspection of the light curves, we discovered ZTF18abhjrcf showing a large (greater than 5 mag) brightness variation over an extended period of time (about 100 days). This is similar to the behavior of the known R Coronae Borealis star. Further spectroscopic follow-up with the Las Cumbres Observatory telescope has confirmed its R Coronae Borealis classification.

11.3. Filter Devkit

The Devkit allows filter authors to develop and test their filter code using real data from the ANTARES database. It is designed to be used in the NOIRLab's DataLab[28] Jupyter environment, where it has direct read-only access to the ANTARES databases. Any user may sign up for Datalab and use the Devkit. The Devkit allows users to fetch Locus data from the database and run filter code on this data in a Python environment that mimics the ANTARES production system, as demonstrated in the following example.

```
import antares.devkit as dk
dk.init() # Initialize the Devkit system
# Define a filter:
class HelloWorld(dk.Filter):
def run(self, locus):
pass
# Run the filter on a random Locus from the database:
dk.run_filter(HelloWorld)
# Run the filter on a specific Locus from the database:
dk.run_filter(HelloWorld, locus_id=...)
```

Users can also construct custom Locus data to test their filters, either by modifying real data or constructing them completely from scratch. The Devkit documentation describes how to do this. Some filters require access to data files such as statistical models, neural networks, lookup tables, etc., as described in Section 6. These data files can be uploaded into

[28] https://datalab.noao.edu/

ANTARES using the Devkit. Full documentation for the Devkit is provided as a standalone website. The Portal's FAQ page provides links to all documentation.

12. ANTARES in the Era of LSST

The data instrument we have described here is already functional at the scale of alerts produced by ZTF. The step to the LSST scale will be at least an order of magnitude greater, if not two. We are confident that the design of the system will scale to match LSST, with only database tuning and hardware expansion necessary to accommodate the larger number of alerts. Specifically, we expect the Cassandra cluster to require significant expansion both for capacity and for throughput. In addition to providing real-time reactivity to alerts, ANTARES will provide a database of all LSST alerts over the operational period and is designed to allow future work on batch processing of this data set. ANTARES will be a general-use broker for the US and world community as it takes advantage of all the time-domain science opportunities that LSST will provide.

The ANTARES team would like to thank the following individuals for their support and advice in the development of this software system: Tim Axelrod, Robert Blum, Todd Boroson, Glenn Eychaner, Mike Fitzpatrick, Michael Fox, Steve Howell, Tim Jenness, Tod Lauer, Nirav Merchant, Catherine Merrill, Robert Nikutta, Knut Olsen, Stephen Ridgway, Robert Seaman, Claire Taylor, Adam Thornton, Jackson Toeniskoetter, Alistair Walker, and John Wregglesworth.

The ANTARES team gratefully acknowledges financial support from the National Science Foundation through a cooperative agreement with the Association of Universities for Research in Astronomy (AURA) for the operation of the NSF's National Optical-Infrared Astronomy Research Laboratory, through an NSF INSPIRE grant to the University of Arizona (CISE AST-1344024, PI: R. Snodgrass), and through a grant from the Heising-Simons Foundation (2018-0909, PI: T. Matheson).

Software: Python[29] (Van Rossum & Drake 2009), Astropy[30] (Astropy Collaboration et al. 2013), Pandas[31] (McKinney 2010; The Pandas Development Team 2020), Kafka,[32] Apache Cassandra,[33] Kubernetes,[34] MySQL,[35] Slack,[36] Elasticsearch,[37] Redis,[38] Lua,[39] JSON[40].

Appendix
Example Filter

This filter selects alerts that have a high signal-to-noise ratio (SNR), based on data intrinsic to the alert itself. Downstream filters can use this information to operate only on those alerts whose detection is more secure.

```
import antares.devkit as dk
class HighSNR(dk.Filter):
ERROR_SLACK_CHANNEL = '' '' # Put author's Slack user ID or
  channel here.
# ˆ This will notify the author if the Filter ever crashes.
# The Filter declares that it does not require any
  LocusProperties.
REQUIRED_LOCUS_PROPERTIES = []
# The Filter declares that it requires the following
  AlertProperties:
REQUIRED_ALERT_PROPERTIES = [
'ant_passband',
'ant_magerr',
]
# The Filter declares that it does not produce output
  LocusProperties.
OUTPUT_LOCUS_PROPERTIES = []
# The Filter declares that it does not produce output
  AlertProperties.
OUTPUT_ALERT_PROPERTIES = []
# The Filter declares that it may produce a Tag called
  ''high_snr''
# and defines a description for it.
OUTPUT_TAGS=[
{
'name': 'high_snr',
'description': 'Locus has one or more Alerts with
  high SNR.',
},
]
def setup(self):
''''''
Declare constants.
'setup()' is called once per Filter per thread, at time of
  system boot.
Filter performance can be optimized by doing as much work
  as possible in
advance in 'setup()'.
eg: loading files, constructing datastructures, etc.,
''''''
# The threshold is dependent on the band that is being
  imaged.
# These threshold values should flag ~2-3% of alerts.
self.snr_threshold = {
'g': 50.0,
'R': 55.0,
}
def run(self, locus):
''''''
If this Alert has a high SNR, then tag the Locus
  "high_snr".
''''''
passband = locus.alert.properties['ant_passband'] #
  Get Alert's band
magerr = locus.alert.properties['ant_magerr'] #
  Get Alert's mag error
if passband not in snr_threshold:
return # This passband is not supported. Do nothing.
threshold = self.snr_threshold[passband] # Get threshold
  for this band
snr = 1.0 / magerr # Compute SNR
if snr > threshold:
locus.tag('high_snr')
```

29 http://python.org
30 http://www.astropy.org
31 https://pandas.pydata.org/
32 https://kafka.apache.org/
33 https://cassandra.apache.org/
34 https://kubernetes.io/
35 https://www.mysql.com/
36 https://slack.com/
37 https://www.elastic.co/
38 https://redis.io/
39 http://www.lua.org/
40 https://www.json.org/json-en.html

ORCID iDs

Thomas Matheson https://orcid.org/0000-0001-6685-0479
Carl Stubens https://orcid.org/0000-0002-2744-714X
Nicholas Wolf https://orcid.org/0000-0002-9508-1629
Chien-Hsiu Lee (李見修) https://orcid.org/0000-0003-1700-5740
Gautham Narayan https://orcid.org/0000-0001-6022-0484
Abhijit Saha https://orcid.org/0000-0002-6839-4881
Adam Scott https://orcid.org/0000-0002-1140-5463
Monika Soraisam https://orcid.org/0000-0001-6360-992X
Adam S. Bolton https://orcid.org/0000-0002-9836-603X
David R. Silva https://orcid.org/0000-0002-7678-2155
John Kececioglu https://orcid.org/0000-0003-1204-6535
Richard Snodgrass https://orcid.org/0000-0003-4703-7460
Patrick D. Aleo https://orcid.org/0000-0002-6298-1663
Zhe Wang https://orcid.org/0000-0002-1720-964X

References

Aartsen, M. G., Ackermann, M., Adams, J., et al. 2017, ApJ, 846, 136
Aasi, J., Abadie, J., Abbott, B. P., et al. 2015, CQGra, 32, 115012
Abbott, B. P., Abbott, R., Abbott, T. D., et al. 2017a, PhRvL, 119, 161101
Abbott, B. P., Abbott, R., Abbott, T. D., et al. 2017b, ApJL, 848, L12
Abbott, B. P., Abbott, R., Abbott, T. D., et al. 2018, LRR, 21, 3
Acernese, F., Agathos, M., Agatsuma, K., et al. 2015, CQGra, 32, 024001
Adrián-Martínez, S., Aguilar, J. A., Samarai, I. A., et al. 2011, ApJL, 743, L14
Aharonian, F., Akhperjanian, A. G., Bazer-Bachi, A. R., et al. 2006, A&A, 457, 899
Alam, S., Albareti, F. D., Allende Prieto, C., et al. 2015, ApJS, 219, 12
Arcavi, I. 2018, ApJL, 855, L23
Astropy Collaboration, Robitaille, T. P., Tollerud, E. J., et al. 2013, A&A, 558, A33
Ayala Solares, H. A., Coutu, S., Cowen, D. F., et al. 2020, APh, 114, 68
Bellm, E. C., Kulkarni, S. R., Graham, M. J., et al. 2019, PASP, 131, 018002
Bianchi, L., Shiao, B., & Thilker, D. 2017, ApJS, 230, 24
Blanton, M. R., Schlegel, D. J., Strauss, M. A., et al. 2005, AJ, 129, 2562
Bloom, J. S., Kasen, D., Shen, K. J., et al. 2012, ApJL, 744, L17
Boch, T., & Fernique, P. 2014, in ASP Conf. Ser. 485, Astronomical Data Analysis Software and Systems XXIII, ed. N. Manset & P. Forshay (San Francisco, CA: ASP), 277
Bonnarel, F., Fernique, P., Bienaymé, O., et al. 2000, A&AS, 143, 33
Borne, K. D. 2008, AN, 329, 255
Cen, R. 2020, ApJL, 888, L14
Chugai, N. 2020, AstL, 46, 319
Corwin, H. G. J., Buta, R. J., & de Vaucouleurs, G. 1994, AJ, 108, 2128
Cutri, R. M., Wright, E. L., Conrow, T., et al. 2014, yCat, 2328, 0
Davenport, J. R. A., Becker, A. C., Kowalski, A. F., et al. 2012, ApJ, 748, 58
De Colle, F., & Lu, W. 2020, NewAR, 89, 101538
de Jaeger, T., Galbany, L., Gutiérrez, C. P., et al. 2018, MNRAS, 478, 3776
de Vaucouleurs, G., de Vaucouleurs, A., Corwin, H. G. J., et al. 1991, Third Reference Catalogue of Bright Galaxies (New York: Springer)
Drake, A. J., Catelan, M., Djorgovski, S. G., et al. 2013a, ApJ, 763, 32
Drake, A. J., Catelan, M., Djorgovski, S. G., et al. 2013b, ApJ, 765, 154
Drake, A. J., Djorgovski, S. G., Catelan, M., et al. 2017, MNRAS, 469, 3688
Drake, A. J., Graham, M. J., Djorgovski, S. G., et al. 2014, ApJS, 213, 9
Drout, M. R., Chornock, R., Soderberg, A. M., et al. 2014, ApJ, 794, 23
Evans, I. N., Primini, F. A., Glotfelty, K. J., et al. 2010, ApJS, 189, 37
Foley, R. J. 2015, MNRAS, 452, 2463
Förster, F., Cabrera-Vives, G., Castillo-Navarrete, E., et al. 2020, arXiv:2008.03303
French, K. D., Arcavi, I., & Zabludoff, A. 2016, ApJL, 818, L21
French, K. D., Arcavi, I., & Zabludoff, A. 2017, ApJ, 835, 176
French, K. D., & Zabludoff, A. I. 2018, ApJ, 868, 99
Gaia Collaboration, Brown, A. G. A., Vallenari, A., et al. 2018, A&A, 616, A1
Gal-Yam, A. 2012, Sci, 337, 927
Gangopadhyay, A., Misra, K., Hiramatsu, D., et al. 2020, ApJ, 889, 170
Gehrels, N., Cannizzo, J. K., Kanner, J., et al. 2016, ApJ, 820, 136
Goldberg, J. A., Bildsten, L., & Paxton, B. 2020, ApJ, 891, 15
Graham, M. J., Kulkarni, S. R., Bellm, E. C., et al. 2019, PASP, 131, 078001
Helou, G., Madore, B. F., Schmitz, M., et al. 1995, ASSL, 203, 95
Holder, J., Atkins, R. W., Badran, H. M., et al. 2006, APh, 25, 391
Hung, T., Foley, R. J., Ramirez-Ruiz, E., et al. 2020, arXiv:2003.09427
Hung, T., Gezari, S., Cenko, S. B., et al. 2018, ApJS, 238, 15
Ivezić, Ž., Kahn, S. M., Tyson, J. A., et al. 2019, ApJ, 873, 111
Jayasinghe, T., Kochanek, C. S., Stanek, K. Z., et al. 2018, MNRAS, 477, 3145
Jayasinghe, T., Stanek, K. Z., Kochanek, C. S., et al. 2019a, MNRAS, 486, 1907
Jayasinghe, T., Stanek, K. Z., Kochanek, C. S., et al. 2019b, MNRAS, 485, 961
Jewitt, D., Hsieh, H., & Agarwal, J. 2015, in Asteroids IV, ed. P. Michel, F. E. DeMeo, & W. F. Bottke (Tucson, AZ: Univ. Arizona Press), 221
Jones, R. L., Slater, C. T., Moeyens, J., et al. 2018, Icar, 303, 181
Juric, M., Jones, R., Moeyens, J., et al. 2017, AAS Meeting, 49, 117.09
Kahn, S. 2018, COSPAR, 42, E1.16-5-18
Kantor, J. 2014, in The Third Hot-wiring the Transient Universe Workshop, ed. P. R. Wozniak et al. (Los Alamos, NM: Los Alamos National Laboratory), 19, http://www.slac.stanford.edu/econf/C131113.1/
Kasliwal, M. M. 2012, PASA, 29, 482
Kasliwal, M. M., Kulkarni, S. R., Arcavi, I., et al. 2011, ApJ, 730, 134
Kasliwal, M. M., Kulkarni, S. R., Gal-Yam, A., et al. 2010, ApJL, 723, L98
Kasliwal, M. M., Kulkarni, S. R., Gal-Yam, A., et al. 2012, ApJ, 755, 161
Khazov, D., Yaron, O., Gal-Yam, A., et al. 2016, ApJ, 818, 3
Knödlseder, J. 2020, arXiv:2004.09213
Kochanek, C. S. 2019, MNRAS, 483, 3762
Komossa, S. 2015, JHEAp, 7, 148
Kulkarni, S. R. 2020, arXiv:2004.03511
Kunszt, P. Z., Szalay, A. S., & Thakar, A. R. 2001, in Proceedings MPA/ESO/MPE Workshop, Mining the Sky, ed. A. J. Banday et al. (Berlin: Springer), 631
Lasker, B. M., Lattanzi, M. G., McLean, B. J., et al. 2008, AJ, 136, 735
Law, N. M., Kulkarni, S. R., Dekany, R. G., et al. 2009, PASP, 121, 1395
Lee, C.-H., Hung, T., Matheson, T., et al. 2020a, ApJL, 892, L1
Lee, C.-H., Matheson, T., Soraisam, M., et al. 2020b, AJ, 159, 61
Margutti, R., Metzger, B. D., Chornock, R., et al. 2019, ApJ, 872, 18
Martini, P., Wagner, R. M., Tomaney, A., et al. 1999, AJ, 118, 1034
Masci, F. J., Laher, R. R., Rusholme, B., et al. 2019, PASP, 131, 018003
McKinney, W. 2010, in Proc. 9th Python in Science Conf., ed. S. van der Walt & J. Millman (Austin, TX: SciPy), 56
Metzger, B. D., & Stone, N. C. 2016, MNRAS, 461, 948
Möller, A., Peloton, J., Ishida, E. E. O., et al. 2021, MNRAS, 501, 3272
Najita, J., Willman, B., Finkbeiner, D. P., et al. 2016, arXiv:1610.01661
Narayan, G., Zaidi, T., Soraisam, M. D., et al. 2018, ApJS, 236, 9
National Research Council 2015, Optimizing the U.S. Ground-Based Optical and Infrared Astronomy System (Washington, DC: The National Academies Press)
Nordin, J., Brinnel, V., van Santen, J., et al. 2019, A&A, 631, A147
Nugent, P. E., Sullivan, M., Cenko, S. B., et al. 2011, Natur, 480, 344
Perets, H. B., Gal-Yam, A., Mazzali, P. A., et al. 2010, Natur, 465, 322
Quimby, R. M., Aldering, G., Wheeler, J. C., et al. 2007, ApJL, 668, L99
Rees, M. J. 1988, Natur, 333, 523
Ridgway, S. T., Matheson, T., Mighell, K. J., Olsen, K. A., & Howell, S. B. 2014, ApJ, 796, 53
Rosen, S. R., Webb, N. A., Watson, M. G., et al. 2016, A&A, 590, A1
Saha, A., Matheson, T., Snodgrass, R., et al. 2014, Proc. SPIE, 9149, 914908
Saha, A., Wang, Z., Matheson, T., et al. 2016, Proc. SPIE, 9910, 99100F
Shappee, B. J., Prieto, J. L., Grupe, D., et al. 2014, ApJ, 788, 48
Skrutskie, M. F., Cutri, R. M., Stiening, R., et al. 2006, AJ, 131, 1163
Smartt, S. J., Clark, P., Smith, K. W., et al. 2018, ATel, 11727, 1
Smith, K. W., Williams, R. D., Young, D. R., et al. 2019, RNAAS, 3, 26
Soraisam, M. D., Saha, A., Matheson, T., et al. 2020, ApJ, 892, 112
Soumagnac, M. T., & Ofek, E. O. 2018, PASP, 130, 075002
The Pandas Development Team 2020, pandas-dev/pandas: Pandas, latest, Zenodo, doi:10.5281/zenodo.3715232
Torrealba, G., Catelan, M., Drake, A. J., et al. 2015, MNRAS, 446, 2251
Trilling, D. E., Valdes, F., Allen, L., et al. 2017, AJ, 154, 170
Van Rossum, G., & Drake, F. L. 2009, Python 3 Reference Manual (Scotts Valley, CA: CreateSpace)
van Velzen, S., Gezari, S., Hammerstein, E., et al. 2020, arXiv:2001.01409
Véron-Cetty, M. P., & Véron, P. 2010, A&A, 518, A10